In Vivo Ultrastructural Localization of the Desmoglein 3 Adhesive Interface to the Desmosome Mid-Line

Atsushi Shimizu, Akira Ishiko, Takayuki Ota, Hitoshi Saito, Hiroshi Oka, Kazuyuki Tsunoda, Masayuki Amagai, and Takeji Nishikawa
Department of Dermatology, Keio University School of Medicine, Tokyo, Japan

Desmoglein (Dsg) is a cadherin cell–cell adhesion molecule located in desmosomes and its precise mechanism for cell–cell adhesion still remains to be elucidated. Opposing cadherin molecules may adhere to the N-terminal EC1 domains, or the entire length of the extracellular (EC) domains may overlap. To solve this controversy, we performed immunoelectron microscopy to map the Dsg3 epitopes in desmosomes. Three different hybridoma cell lines producing anti-Dsg3 monoclonal antibodies (mAb) were intraperitoneally injected into immunodeficient mice and the precise ultrastructural location of bound IgG between the mucosal epithelial cells *in vivo* was statistically measured and analyzed. The binding site of the AK23 mAb that recognizes the N-terminal EC1 domain was localized to the electron-dense mid-line of desmosomes. The binding sites of AK7 and AK18, which recognize the C-terminal membrane proximal and middle portions of the EC domains, were localized to the desmosomal region proximal to the membrane and the region between the plasma membrane and the dense mid-line, respectively. These results indicate that the N-terminal regions of Dsg3 from opposing cells interact at the dense mid-line of desmosomes where EC1 overlaps.

Key words: adhesion molecule/cadherin/immunoelectron microscopy/pemphigus vulgaris
J Invest Dermatol 124:984–989, 2005

Desmosomes are well known to provide reinforced and sustained cell–cell adhesion in epithelia and cardiac muscle. Ultrastructurally, desmosomes form symmetrical, disc-like junctions that link the intermediate filaments or tono filaments within cells to the plasma membrane and to adjacent cells (Kelly and Shienvold, 1976). The intercellular region of the desmosome, the desmoglea, shows a constant structure, comprising a dense mid-line and electron-dense bridges extending between the mid-line and the plasma membrane. The intracellular (cytoplasmic) structure of desmosomes consists of a double plaque, an extremely dense outer plaque and a less dense inner plaque that joins the tonofilaments. The maximum average size of desmosome is 0.5 μm or less in diameter, and the width of the intercellular space is approximately 30 nm (North *et al*, 1999; He *et al*, 2003). Desmosomes contain two subfamilies of desmosomal cadherins, the desmogleins (Dsg) and desmocollins; the most important of these are expressed in a cell-type and differentiation-specific pattern (Schmidt *et al*, 1994; Kurzen *et al*, 1998; Getsios *et al*, 2004). Desmosomal cadherins belong to the most closely related branches of the cadherin superfamily, such as the classical cadherins (E-, N-, and P-cadherin), and these transmembrane proteins are characterized by the presence of five tandem, independently folding extracellular (EC) domains (EC1 to EC5) that contain the highly conserved calcium-binding motifs (Ozawa *et al*, 1990; Nollet *et al*, 2000; Garrod *et al*, 2002). Dsg3 has been shown to be the antigen recognized by autoantibodies from patients with pemphigus vulgaris (PV), a life-threatening autoimmune blistering disease affecting the skin and mucous membranes (Amagai *et al*, 1991; Stanley, 1993). Previously, a novel PV experimental murine model was generated by adoptive transfer of splenocytes from mDsg3-immunized Dsg3−/− mouse to Rag2−/− immunodeficient mice that normally express Dsg3 (Amagai *et al*, 2000). These model mice stably produced anti-Dsg3 IgG and developed the characteristic features of PV (Ohyama *et al*, 2002; Shimizu *et al*, 2002). Furthermore, by immunoelectron microscopy (EM), these model mice clearly demonstrated IgG deposition within the EC portion of desmosomes and showed split-desmosomes without keratin filament retraction. These results produced speculation that the autoantibody binding to Dsg3 in the desmosome causes desmosomal splitting by direct inhibition of the adhesive function(s) of Dsg3 in PV (Shimizu *et al*, 2004).

Cadherin EC region consists of five EC domains numbered from the outermost N-terminal domain (Fig 1*a*). The so-called cell adhesion recognition site (CAR site), which was reported by Blaschuk *et al* (1990), is a highly conserved amino acid sequence located in the EC1 domain. This sequence is indispensable for cell adhesion (Nose *et al*, 1990; Noe *et al*, 1999), which can be specifically blocked by short peptides corresponding CAR sites (Tselepis *et al*, 1998), and is different between the various desmosomal cadherins, although these sequences are largely conserved between

Abbreviations: CAR, cell adhesion recognition; Dsg, desmoglein; EC, extracellular; EM, electron microscopy; mAb, monoclonal antibody; PV, pemphigus vulgaris

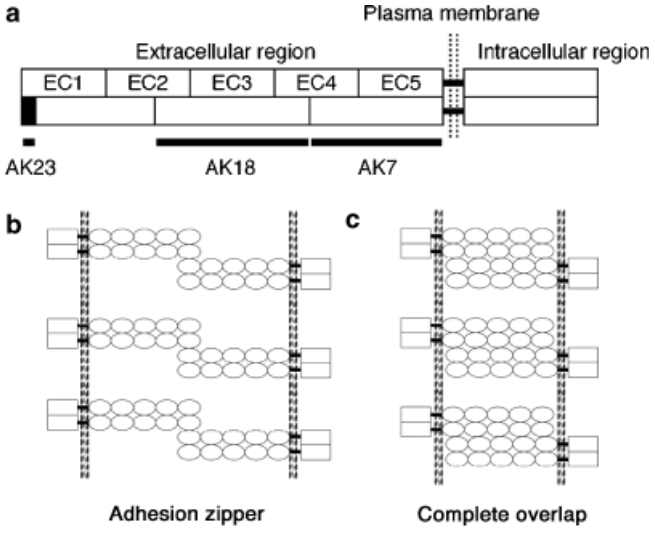

Figure 1
The molecular structure and cadherin desmosome adhesion models. The cadherin extracellular (EC) region consists of five EC domains numbered from the outermost N-terminal domain. The monoclonal antibody epitopes used in the study are indicated by bars on the diagram *a*. Diagram *b* shows the proposed *trans*-binding interaction by the outermost domains (adhesion zipper model). Diagram *c* shows a completely interdigitated protein model (complete overlap model).

homologous molecules from different species. So far, the precise molecular mechanisms of cadherin cell adhesion are still controversial as Garrod *et al* (2002) discussed in a recent review paper. For the classical cadherins, previous structural work has suggested that the CAR site forms part of the adhesive interface and an "adhesion zipper" model (Fig 1*b*) has thus been proposed (Shapiro *et al*, 1995). This model suggests cadherin molecules form strand dimers in *cis*-formation and adhesion dimers in a *trans*-orientation, with adhesion taking place between the EC1 domains of the apposed molecules. Another model of cadherin adhesion is the "complete overlap" model (Fig 1*c*). Using surface force apparatus to quantify the interactions between recombinant E-cadherin EC domains, Sivasankar *et al* (1999, 2001) showed that adhesion was greatest when the overlap of these molecules was complete. This model was supported by Chappuis-Flament *et al* (2001) using a bead aggregation assay and a cell attachment-based assay with a series of domains lacking recombinant proteins. There have been no reports of desmosomal cadherin adhesion until a recent structural study using electron tomography suggested a model forming discrete groups and interacting through the molecular tips of opposing cadherins (He *et al*, 2003). The interpretation of the results, however, was based on simply applying or overlaying the C-cadherin crystal structure to the desmosomal ultrastructural micrographs. More structural studies on intact desmosomes are urgently needed to clarify the relationship between the desmosomal structure and this molecular interaction. More recently, we have characterized several AK series monoclonal antibodies (mAb) against Dsg3, including AK7, AK18, and AK23, from active PV mice models. The epitopes recognized by AK7 and AK18, which lacked apparent pathogenic activities using a hybridoma inoculation assay, were mapped to the carboxyl-terminal region and the middle region of the EC domain of the Dsg3, respectively. It is particularly noteworthy that the clone AK23, the epitope of which was located in residues 1–63 of the EC1 domain, possessed pathogenic activities and could readily induce suprabasal acantholysis by intraperitoneal injection to the adult mice. Subsequent extensive studies with point-mutated Dsg1/Dsg3 molecules revealed that AK23 recognized a conformational epitope that comprises the V3, K7, P8, and D59 residues, which are precisely located on the Dsg3-specific adhesive interface (Tsunoda *et al*, 2003).

The goal of this study was to characterize the *in vivo* ultrastructural localization of the cell adhesion site on Dsg3 in epithelial desmosomes and to precisely map the Dsg3 molecule using immuno-EM. Here we show that the cell adhesion site of Dsg3, the epitope of AK23, localized to the dense mid-line whereas the locations of epitopes of AK7 or AK18 lay within the C-terminal or the middle portion of the Dsg3 EC domain, respectively, and provide the first *in vivo* evidence of desmosomal Dsg3 EC1 interactions between adjacent keratinocytes.

Results

The cell adhesion interface of Dsg3 is on the dense midline of the desmosome All sera from hybridoma cell-inoculated mice reacted with the keratinocyte cell surfaces of the hard palate of normal mice by indirect immunofluorescence, indicating the production of anti-Dsg3 antibodies

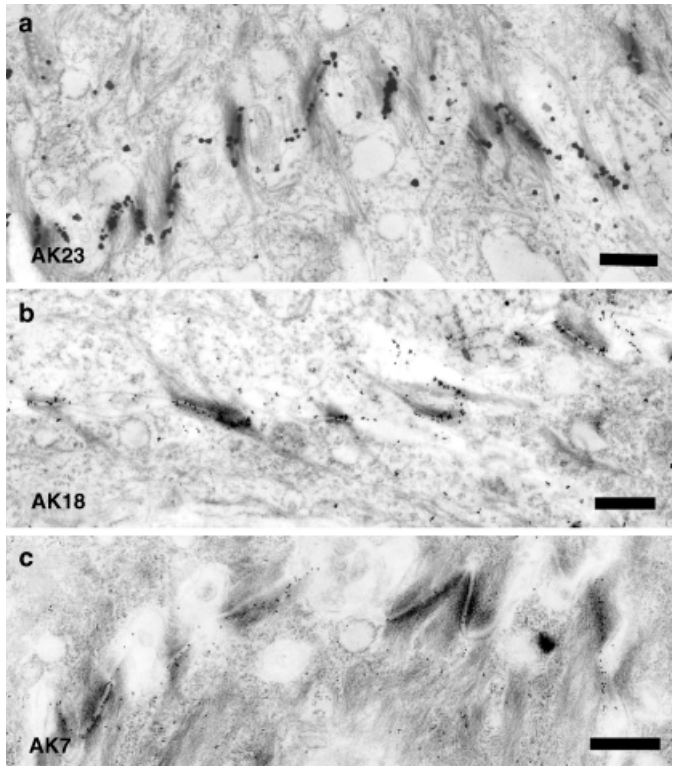

Figure 2
All AK monoclonal antibodies bound to the desmosome. For low-power electron microscopy magnification view, sections of hard palate epithelia from hybridoma-inoculated mice were incubated with rabbit anti-mouse IgG followed by gold-conjugated anti-rabbit IgG, and enhanced by silver staining. Note that the labeling was concentrated at sites of desmosomes attachment plaques. (*a*) AK23, (*b*) AK18, and (*c*) AK7. *Scale bars* = 500 nm.

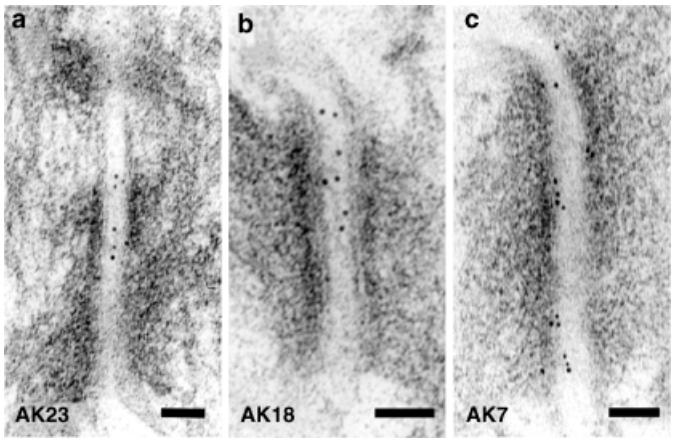

Figure 3
The AK23 epitope was localized to the dense mid-line, whereas AK7 and AK18 epitopes were localized near the plasma membrane in the extracellular (EC) portion of desmosome. For a high-power electron microscopy magnification view, sections of hard palate epithelia from hybridoma-inoculated mice were incubated with rabbit anti-mouse IgG followed by 5 nm gold anti-rabbit IgG. The majority of all AK monoclonal antibodies were observed over the EC portion of desmosomes. AK23 was mainly localized at the midpoint between the attachment plaques of desmosomes close to the dense mid-line (*a*) AK18 was localized between the attachment plaques of desmosomes and the dense midline (*b*) AK7 was localized to near the plasma membrane of the EC portion of desmosomes (*c*). *Scale bars* = 50 nm.

(data not shown). By direct immunofluorescence, all the inoculated mice showed IgG deposition at the keratinocyte cell surfaces of the hard palate (data not shown), similar to the previous experiment (Tsunoda *et al*, 2003). To determine the ultrastructural localization of these *in vivo*-bound IgG molecules, post-embedding immunogold EM was performed. Low-magnification views of each AK mAb-inoculated mouse after significant silver enhancement demonstrated that labeling of AK mAb was mainly localized to the desmosome (Fig 2). Some labeling in the cytoplasm was thought to be background binding of anti-mouse IgG secondary antibodies because similar labeling was observed in all mice including the control mice, which had not undergone hybridoma inoculation (data not shown). High-magnification views without silver enhancement demonstrated that all the AK mAb were specifically deposited between the attachment plaques of the desmosome, i.e. in the EC region of the desmosome (Fig 3). Upon closer observation, the binding sites of AK23, AK18, and AK7 mAb were slightly different. The respective binding sites were located along the dense mid-line (Fig 3*a*), between the dense mid-line and plasma membrane (Fig 3*b*), or near the plasma membrane (Fig 3*c*). By careful measurement of the distance from a single gold particle to the inner layer of the plasma membrane, the distributions of 296 gold particles that labeled AK23 and 328 gold particles that labeled AK7 or AK18 epitope in each mAb were plotted on the histogram (Fig 4). In each mAb, almost all labeling was located within the EC region of the desmosome. More than 30 percent of labeling for AK23 formed a single, narrow, sharp peak at the midpoint between the EC region of the desmosome over the dense mid-line and the frequency of labeling gradually decreased approaching the desmosomal plasma membrane. The histogram of AK23 antibodies showed a normal distribution. The best-fit curve for AK23 antibodies was calcu-

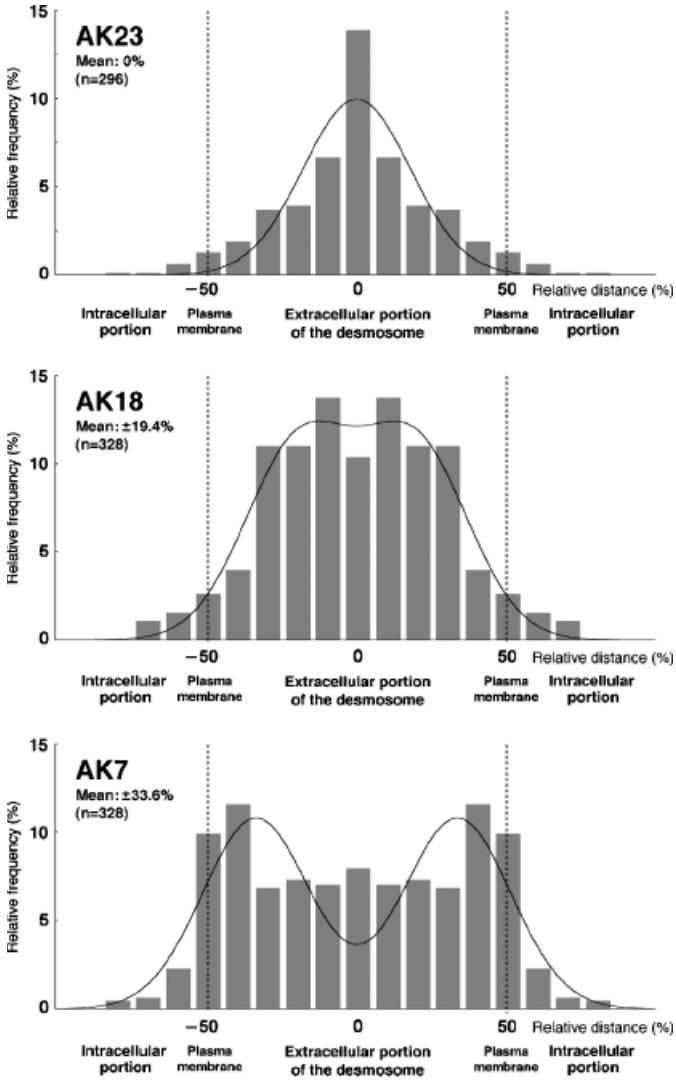

Figure 4
The distribution of the monoclonal antibodies epitopes in the desmosome from hybridoma-inoculated mice. To calculate the distance from the plasma membrane, histograms were obtained by measuring the distance between the gold particles and the middle of the desmosome. AK23 showed a major single peak at the center of desmosomes where a dense mid-line exists and more than 30% of the labeling was associated with this regional peak, indicating that the AK23 epitope is restricted to the dense mid-line of the desmosome. The AK23 antibody histogram showed a normal distribution. The best-fit curve for AK23 antibodies was calculated from a normal distribution curve and its standard deviation was 17.8 (percentage relative distance) (*a*) In contrast, AK18 formed double peaks near the mid point of the extracellular (EC) portion of desmosomes (*b*). The mAb AK7 also formed twin peaks near the plasma membrane at the EC portion of desmosomes. Approximated curves for AK18 and AK7 histograms were drawn with the sum of two functions, which had different-signed (+/−) mean values, but the same standard deviation as the AK23 antibody. The average vertical distances from the midline were calculated to be 19.4% and 33.6%, respectively, for AK7 and AK18 antibody.

lated from normal distribution curve and its standard deviation was 17.8 (percentage relative distance). In contrast, the distribution of AK18 and AK7 epitopes formed double peaks and an M-shaped distribution, with the location of the peaks mid-way between dense mid-line and plasma membranes, or near the plasma membrane, respectively. Approximated curves for AK18 and AK7 histograms were drawn with the sum of two functions, which had

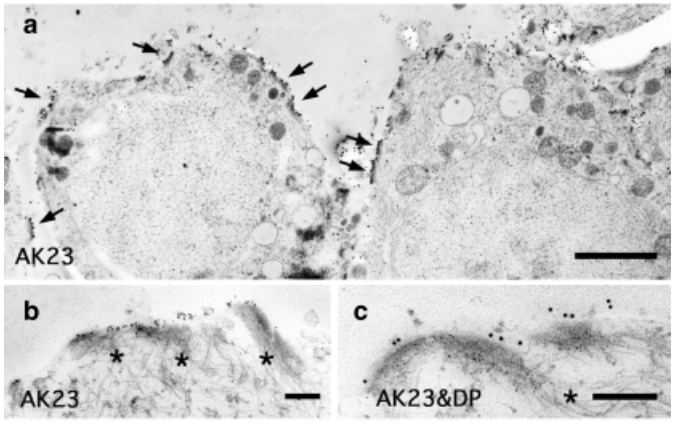

Figure 5
On the split-desmosomes caused by AK23 hybridoma-inoculation, the AK23 epitope could be localized at the extracellular (EC) portion without keratin filaments retraction. Acantholysis is observed in the suprabasal layer of the AK23 hybridoma-inoculated mice. Separated acantholytic cells retained several split-desmosomes on the cell surface where decoration desmosomes with gold particles that recognized AK23 monoclonal antibodies could be seen (arrows) (*a*). Under high-power electron microscopy magnification, AK23 was exclusively localized at the EC portion of split-desmosomes, but no labeling was observed in the interdesmosomal areas (*b*). By double labeling, AK23 (15 nm gold) and desmoplakin (5 nm gold) were localized at the EC portion of the desmosome and at the junction between the desmosomal attachment plaque and keratin filaments, respectively (*c*). *, keratin filaments. *Scale bars* = 1 μm (*a*) and 200 nm (*b* and *c*).

different-signed mean values, but were assumed to have the same standard deviation as AK23 antibodies. The average vertical, relative distances from the mid-line were calculated to be 19.4 (%) and 33.6 (%), respectively, for AK7 and AK18 antibody. If the distance between the plasma membranes in a desmosome is 30 nm, the location of epitopes of AK7 and AK18 can be calculated to be 5.8 and 10.1 nm, respectively, from the dense mid-line.

The mAb AK23 leads to the desmosomal splitting without keratin filament retraction After inoculation with the AK23 mAb hybridoma cells alone (not AK7 nor AK18), mice developed a PV phenotype including oral erosions and suprabasal acantholysis as previously described (Tsunoda *et al*, 2003). By observing the apical surface of acantholytic basal cells of these mice, separated keratinocytes retained many split-desmosomes that were labeled by anti-mouse IgG (Fig 5*a*). High-magnification views showed the EC localization of IgG on the split-desmosome (Fig 5*b*). Double-immunogold labeling of the sections demonstrated that AK23 (using a 15 nm gold probe) localized the EC portion of the split-desmosome, whereas desmoplakin (5 nm gold) distributed widely between the outer attachment plaque and keratin filaments (Fig 5*c*).

Discussion

Recent biochemical and ultrastructural studies have shown that the EC cadherin regions can interact with one another in diverse ways. They may form the adhesive interface between the EC1 domains in a *trans*-interacting manner with other adhesion molecules (Overduin *et al*, 1995; Shapiro *et al*, 1995), or they may form hydrophobic pockets for docking utilizing the conserved amino-terminal side-chain tryptophan residue (Pertz *et al*, 1999). But it has been questioned whether interaction between the EC1 domains alone is sufficient to mediate classical cadherin adhesion, and a more extensive overlap between the EC domains has been proposed (Sivasankar *et al*, 1999, 2001; Chappuis-Flament *et al*, 2001). As to the desmosomal cadherins, Rayns' *et al* (1969) showed more than 30 y ago using a lanthanum infiltration technique that the electron-dense mid-line, which exists between the two cells desmosomal attachment plaques, appeared as a zigzag, the apices of which were structurally connected to the nearer plasma membrane. Recently, He *et al* (2003) revealed the three-dimensional structure between the attachment plaques using electron tomography, a modern sophisticated electron microscopic technique. It was shown that individual molecules formed discrete groups and interacted through their distal tips. Thus, there is a concentration of protein at the mid-line that bridges the two plasma membranes. Molecular interpretation of these results, however, was based upon the C-cadherin crystal structure but not the desmosomal cadherins, and there has been no direct evidence to show the molecular composition of the dense mid-line. Although the end terminal domains of desmosomal cadherins, including CAR sites, have been shown to be involved in cell adhesion and positioning using peptide inhibitory experiments (Tselepis *et al*, 1998; Runswick *et al*, 2001), their *in situ* ultrastructural localization in desmosomes has not been elucidated. In this study, we have directly immunolocalized the AK23 epitope, which forms the molecular binding interface, at the dense mid-line of the desmosome for the first time. Moreover, ultrastructural mapping suggested the linear structure of the Dsg3 ectodomain: AK18 in the EC2-4 domain localizing 5.8 nm from the mid-line (between the plasma membrane and the dense mid-line) and AK7 in EC4-5 localizing 10.1 nm from the mid-line (near the plasma membrane). There is a possibility that binding of AK23 antibody to the Dsg3 *in vivo* may change the structure of Dsg3 and the labeling may not represent the *in situ* localization of the EC1 domain. The best way to check this possibility was to perform on-section AK23 labeling on normal mouse epithelium; however, this approach was unsuccessful. This may be because the AK23 epitope is localized on the adhesive interface and is not exposed for antibody penetration in the specimen in which Dsg3 is immobilized by resin embedding. We have previously shown that the on-section labeling pattern of PV model mouse serum on the normal mouse epithelia and the distribution of *in vivo* binding IgG in the PV model mouse are almost identical (Shimizu *et al*, 2004). Therefore, it is unlikely that any major conformational changes have occurred on Dsg3, despite autoantibodies bound to their respective EC epitopes.

It is well known that IgG autoantibodies alone can induce blister formation in the skin and mucous membranes of PV model mice. Keratin retraction from the attachment plaque is also a well-known phenomenon in cultured keratinocytes exposed to the Dsg3 autoantibodies. In this study, acantholysis was observed in the AK23 hybridoma inoculated mice. At the acantholytic area, splitting of desmosomes was seen in a manner similar to the previous reports of PV model mice (Shimizu *et al*, 2002, 2004). Even in these

split-desmosomes, keratin filaments were still in contact with the attachment plaque via desmoplakin. Considering the fact that AK23 epitope involves functionally critical residues for cell adhesion, our data further support the notion that a spatial steric interference of EC1 interactions by IgG binding causes the physical splits of desmosomes as an initial event of acantholysis followed by keratin retraction.

Material and Methods

Production and epitope mapping of anti-Dsg3 mAb We had previously identified eight anti-Dsg3 clone mAb generated from the PV model mice (Tsunoda *et al*, 2003) and three of them AK7, AK18, and AK23 were used in this study. All mAb had the IgG1 isotype for the H chain and the κ isotype for the L chain. The epitopes of these anti-Dsg3 mAb have also been determined by immunoprecipitation using domain-swapped or point-mutated Dsg1/Dsg3 molecules. The AK7 epitope appears to reside between residue 403 in domain EC4 and residue 565 in domain EC5 of mouse Dsg3, which represents the C-terminal portion of the EC domain. The AK18 mAb appears to bind between residues 195 in EC2 and 402 in EC4 of mouse Dsg3, which represents the middle portion of the EC domain. Lastly, the epitope AK23 mAb appears to recognize residues 1–63 in mouse Dsg3, which represents the N-terminal end portion of the EC domain. Furthermore, AK23 mAb showed pathogenic activities by causing the formation of ascites in adult mice and recognized a calcium-dependent conformational epitope that consisted of the V3, K7, P8, and D59 at the N terminus of mDsg3 (Tsunoda *et al*, 2003). Schematic diagrams of the epitopes recognized by these three mAb in the Dsg3 molecule are summarized in Fig 1*a*.

Intraperitoneal inoculation of AK hybridoma cells We performed a hybridoma inoculation assay to immunolabel Dsg3 in the desmosomes as well as to evaluate the pathogenic activities of AK mAb in adult mice, as described elsewhere (Tsunoda *et al*, 2003). In brief, we inoculated i.p. 5×10^6 hybridoma cells of each AK mAb clone into in Rag2$-/-$ mice that were primed with 2, 6, 10, 14-tetramethyl-pentadecane (Wako Pure Chemical Industries, Osaka, Japan). The inoculated mice were monitored for ascites formation as well as the appearance of the PV phenotype. Biopsies of the oral mucous membranes and skin were taken on day 14 when ascites formation was observed in all mice and the PV phenotype was observed in AK23-inoculated mice. All mouse studies were approved by the animal ethics review board of Keio University.

Immunofluorescence Cryosections of unfixed oral mucous membrane from these hybridoma-inoculated mice were stained with rabbit anti-mouse immunoglobulins conjugated with fluorescein isothiocyanate (FITC) (DAKO, Copenhagen, Denmark) at room temperature for 1 h and viewed under an epifluorescence microscope. For the control study, oral mucous membranes of Rag2$-/-$ mice without cell inoculation were used as a substrate instead of the samples from AK mAb-inoculated mice.

Low-temperature immuno EM Samples for low-temperature immuno-EM were isolated from the oral mucous membranes of AK mAb-inoculated mice and Rag2$-/-$ mice, and post-embedding immuno-EM was performed as previously described (Shimizu *et al*, 1989). In brief, small pieces (<1 mm^2) of mucous membrane samples were cut and cryofixed by rapidly plunging them into liquid propane (-190°C) and cryosubstituted in pure methanol for 48 h at -80°C followed by embedding in Lowicryl K11M (Ladd Research Ind, Williston, Vermont) at -60°C. Specimens were polymerized with UV radiation at -60°C for 48 h and at room temperature for another 48 h. The ultrathin sections were cut vertically to the skin surface, collected on nickel grids covered with a polyvinyl formvar support film, and processed for immunogold labeling. The ultrathin sections were immunolabeled with affinity-purified rabbit anti-mouse IgG (H + L) (American Qualex Antibodies, San Clemente, California) and 5 or 15 nm colloidal gold-conjugated goat anti-rabbit IgG (Amersham Life Science, Olen, Belgium). For low-power EM, the colloidal gold probes were amplified with the IntenSE silver enhancement kit (Amersham). Double-sided immunolabeling with anti-desmoplakin antibodies was performed, as described previously (Shimizu *et al*, 2004). For the control study, oral mucous membrane of Rag2$-/-$ mice was used as a substrate instead of the samples from these mAb hybridoma-inoculated mice.

Quantitative analysis of the immuno-EM The immunoelectron micrographs were scanned at a high resolution and analyzed using Image-Pro Plus (Media Cybernetics, Silver Spring, Maryland) as described previously (Shimizu *et al*, 2004). The distance or thickness (in nm) between the two desmosomal plasma membranes (L1) and the distance between a single gold particle to the midpoint of L1 (L2) were measured in pairs (for each cells plasma membrane) for more than 300 gold particles. The data for the vertical length were calculated as the relative distance according to the following formula: L2/L1 $\times$ 100, and plotted as a histogram. The best-fit curve for each antibody histogram was calculated using the least mean square approximation calculated by C program.

This work was supported by Health and Labor Sciences Research Grants for Research on Measures for Intractable Diseases, from the Ministry of Health, Labor, and Welfare, and by Grant-in Aids for Scientific Research and for the Development of Innovative Technology from the Ministry of Education, Culture, Sports, Science and Technology of Japan. We would like to thank Toshihiko Nagai for their technical assistance and Dr James R. McMillan for the critical reading of this manuscript.

DOI: 10.1111/j.0022-202X.2005.23706.x

Manuscript received September 8, 2004; revised December 28, 2004; accepted for publication January 3, 2005

Address correspondence to: Akira Ishiko, Department of Dermatology, Keio University School of Medicine, 35 Shinanomachi, Shinjuku, Tokyo, 160-8582, Japan. Email: ishiko@sc.itc.keio.ac.jp

References

Amagai M, Klaus-Kovtun V, Stanley JR: Autoantibodies against a novel epithelial cadherin in pemphigus vulgaris, a disease of cell adhesion. Cell 67: 869–877, 1991

Amagai M, Tsunoda K, Suzuki H, Nishifugi K, Koyasu S, Nishikawa T: Use of autoantigen-knockout mice in developing an active autoimmune disease model for pemphigus. J Clin Invest 105:625–631, 2000

Blaschuk OW, Sullivan R, David S, Pouliot Y: Identification of a cadherin cell adhesion recognition sequence. Dev Biol 139:227–229, 1990

Chappuis-Flament S, Wong E, Hicks LD, Kay CM, Gumbiner BM: Multiple cadherin extracellular repeats mediate homophilic binding and adhesion. J Cell Biol 154:231–243, 2001

Garrod DR, Merritt AJ, Nie Z: Desmosomal adhesion: Structural basis, molecular mechanism and regulation (review). Mol Membrane Biol 19:81–94, 2002

Getsios S, Huen AC, Green KJ: Working out the strength and flexibility of desmosomes. Nat Rev Mol Cell Biol 5:271–281, 2004

He W, Cowin P, Stokes DL: Untangling desmosomal knots with electron tomography. Science 302:109–113, 2003

Kelly DE, Shienvold FL: The desmosome: Fine structural studies with freeze-fracture replication and tannic acid staining of sectioned epidermis. Cell Tissue Res 172:309–323, 1976

Kurzen H, Moll I, Moll R, *et al*: Compositionally different desmosomes in the various compartments of the human hair follicle. Differentiation 63: 295–304, 1998

Noe V, Willems J, Vandekerckhove J, Roy FV, Bruyneel E, Mareel M: Inhibition of adhesion and induction of epithelial cell invasion by HAV-containing E-cadherin-specific peptides. J Cell Sci 112:127–135, 1999

Nollet F, Kools P, van Roy F: Phylogenetic analysis of the cadherin superfamily allows identification of six major subfamilies besides several solitary members. J Mol Biol 299:551–572, 2000

North AJ, Bardsley WG, Hyam J, *et al*: Molecular map of the desmosomal plaque. J Cell Sci 112:4325–4336, 1999

Nose A, Tsuji K, Takeichi M: Localization of specificity determining sites in cadherin cell adhesion molecules. Cell 61:147–155, 1990

Ohyama M, Amagai M, Tsunoda K, *et al*: Immunologic and histophathologic characterization of active disease mouse model for pemphigus vulgaris. J Invest Dermatol 118:199–204, 2002

Overduin M, Harvey TS, Bagby S, Tong KI, Yau P, Takeichi M, Ikura M: Solution structure of the epithelial cadherin domain responsible for selective cell adhesion. Science 267:386–389, 1995

Ozawa M, Engel J, Kemler R: Single amino acid substitutions in one Ca^{2+} binding site of uvomorulin abolish the adhesive function. Cell 63:1033–1038, 1990

Pertz O, Bozic D, Koch AW, Fauser C, Brancaccio A, Engel J: A new crystal structure, Ca^{2+} dependence and mutational analysis reveal molecular details of E-cadherin homoassociation. EMBO J 18:1738–1747, 1999

Rayns DG, Simpson FO, Ledingham JM: Ultrastructure of desmosomes in mammalian intercalated disc; appearances after lanthanum treatment. J Cell Biol 42:322–326, 1969

Runswick SK, O'Hare MJ, Jones L, Streuli CH, Garrod DR: Desmosomal adhesion regulates epithelial morphogenesis and cell positioning. Nat Cell Biol 3:823–830, 2001

Schmidt A, Heid HW, Schafer S, Nuber UA, Zimbelmann R, Franke WW: Desmosomes and cytoskeletal architecture in epithelial differentiation: Cell type-specific plaque components and intermediate filament anchorage. Eur J Cell Biol 65:229–245, 1994

Shapiro L, Fannon AM, Kwong PD, *et al*: Structural basis of cell–cell adhesion by cadherins. Nature 374:327–337, 1995

Shimizu A, Ishiko A, Ota T, Tsunoda K, Amagai M, Nishikawa T: IgG binds to desmoglein 3 in desmosomes and causes a desmosomal split without keratin retraction in a pemphigus mouse model. J Invest Dermatol 122:1145–1153, 2004

Shimizu A, Ishiko A, Ota T, Tsunoda K, Koyasu S, Amagai M, Nishikawa T: Ultrastructural changes in mice actively producing antibodies to desmoglein 3 parallel those in patients with pemphigus vulgaris. Arch Dermatol Res 294:318–323, 2002

Shimizu H, McDonald JN, Kennedy AR, Eady RA: Demonstration of intra- and extracellular localization of bullous pemphigoid antigen using cryofixation and freeze substitution for postembedding immunoelectron microscopy. Arch Dermatol Res 281:443–448, 1989

Sivasankar S, Brieher W, Lavrik N, Gumbiner B, Leckband D: Direct molecular force measurements of multiple adhesive interactions between cadherin ectodomains. Proc Natl Acad Sci USA 96:11820–11824, 1999

Sivasankar S, Gumbiner B, Leckband D: Direct measurements of multiple adhesive alignments and unbinding trajectories between cadherin extracellular domains. Biophys J 80:1758–1768, 2001

Stanley JR: Cell adhesion molecules as targets of autoantibodies in pemphigus and pemphigoid, bullous diseases due to defective epidermal cell adhesion. Adv Immunol 53:291–325, 1993

Tselepis C, Chidgey M, North A, Garrod D: Desmosomal adhesion inhibits invasive behavior. Proc Natl Acad Sci USA 95:8064–8069, 1998

Tsunoda K, Ota T, Aoki M, *et al*: Induction of pemphigus phenotype by a mouse monoclonal antibody against the amino-terminal adhesive interface of desmoglein 3. J Immunol 170:2170–2178, 2003